



Article

# Developing Folate-Conjugated miR-34a Therapeutic for Prostate Cancer: Challenges and Promises

Wen (Jess) Li <sup>1,2,\*</sup>, Yunfei Wang <sup>1</sup>, Xiaozhuo Liu <sup>1</sup>, Shan Wu <sup>1</sup>, Moyi Wang <sup>1</sup>, Steven G. Turowski <sup>3</sup>, Joseph A. Spornyak <sup>3</sup>, Amanda Tracz <sup>1</sup>, Ahmed M. Abdelaal <sup>4</sup>, Kasireddy Sudarshan <sup>4</sup>, Igor Puzanov <sup>5</sup>, Gurkamal Chatta <sup>5</sup>, Andrea L. Kasinski <sup>4</sup> and Dean G. Tang <sup>1,2,\*</sup>

<sup>1</sup> Department of Pharmacology and Therapeutics, Roswell Park Comprehensive Cancer Center, Buffalo, NY 14263, USA; wangyunfei@mail.jnmc.edu.cn (Y.W.); xiaozhuo.liu@roswellpark.org (X.L.); shan.wu@roswellpark.org (S.W.); moyi.wang@roswellpark.org (M.W.)

<sup>2</sup> Experimental Therapeutics (ET) Graduate Program, Roswell Park Comprehensive Cancer Center and the University at Buffalo, Buffalo, NY 14263, USA

<sup>3</sup> Department of Cell Stress Biology, Roswell Park Comprehensive Cancer Center, Buffalo, NY 14263, USA

<sup>4</sup> Department of Biological Sciences, Purdue University, West Lafayette, IN 47907, USA

<sup>5</sup> Department of Medicine, Roswell Park Comprehensive Cancer Center, Buffalo, NY 14263, USA

\* Correspondence: wen.li@roswellpark.org (W.L.); dean.tang@roswellpark.org (D.G.T.)

**Abstract:** Prostate cancer (PCa) remains a common cancer with high mortality in men due to its heterogeneity and the emergence of drug resistance. A critical factor contributing to its lethality is the presence of prostate cancer stem cells (PCSCs), which can self-renew, long-term propagate tumors, and mediate treatment resistance. MicroRNA-34a (miR-34a) has shown promise as an anti-PCSC therapeutic by targeting critical molecules involved in cancer stem cell (CSC) survival and functions. Despite extensive efforts, the development of miR-34a therapeutics still faces challenges, including non-specific delivery and delivery-associated toxicity. One emerging delivery approach is ligand-mediated conjugation, aiming to achieve specific delivery of miR-34a to cancer cells, thereby enhancing efficacy while minimizing toxicity. Folate-conjugated miR-34a (folate-miR-34a) has demonstrated promising anti-tumor efficacy in breast and lung cancers by targeting folate receptor  $\alpha$  (FOLR1). Here, we first show that miR-34a, a TP53 transcriptional target, is reduced in PCa that harbors TP53 loss or mutations and that miR-34a mimic, when transfected into PCa cells, downregulated multiple miR-34a targets and inhibited cell growth. When exploring the therapeutic potential of folate-miR-34a, we found that folate-miR-34a exhibited impressive inhibitory effects on breast, ovarian, and cervical cancer cells but showed minimal effects on and targeted delivery to PCa cells due to a lack of appreciable expression of FOLR1 in PCa cells. Folate-miR-34a also did not display any apparent effect on PCa cells expressing prostate-specific membrane antigen (PSMA) despite the reported folate's binding capability to PSMA. These results highlight challenges in the specific delivery of folate-miR-34a to PCa due to a lack of target (receptor) expression. Our study offers novel insights into the challenges and promises within the field and casts light on the development of ligand-conjugated miR-34a therapeutics for PCa.

**Keywords:** microRNA-34a; microRNA; prostate cancer; folate receptor; PSMA; miRNA therapeutics; cancer stem cells; miRNA ligand conjugates



**Citation:** Li, W.; Wang, Y.; Liu, X.; Wu, S.; Wang, M.; Turowski, S.G.; Spornyak, J.A.; Tracz, A.; Abdelaal, A.M.; Sudarshan, K.; et al. Developing Folate-Conjugated miR-34a Therapeutic for Prostate Cancer: Challenges and Promises. *Int. J. Mol. Sci.* **2024**, *25*, 2123. <https://doi.org/10.3390/ijms25042123>

Academic Editors: Francesca Sanguedolce, Hiroshi Miyamoto and Giuseppe Lucarelli

Received: 27 November 2023

Revised: 30 January 2024

Accepted: 5 February 2024

Published: 9 February 2024



**Copyright:** © 2024 by the authors. Licensee MDPI, Basel, Switzerland. This article is an open access article distributed under the terms and conditions of the Creative Commons Attribution (CC BY) license (<https://creativecommons.org/licenses/by/4.0/>).

## 1. Introduction

Prostate cancer (PCa) remains a formidable challenge in men due to its remarkable heterogeneity and the emergence of drug resistance, resulting in ultimately lethal castration-resistant prostate cancer called CRPC. This malignancy, characterized by multiple distinct cancer foci and varying androgen receptor (AR) expression levels, has been at the forefront of therapeutic research for decades. The current standard-of-care therapies, including androgen receptor signaling inhibitors (ARSIs), radiotherapy, and chemotherapies, have

exhibited good clinical efficacy, but offer survival benefits only measured in months in advanced PCa patients [1,2]. A critical factor contributing to ARSI resistance and therapeutic failure is the existence of prostate cancer stem cells (PCSCs), a subpopulation of cells within the tumor that possess stem cell traits [3,4]. These PCSCs can long-term self-renew, propagate tumors *in vivo*, and are inherently ARSI-refractory. In addition, tumor progression and therapeutic treatments may induce plasticity by reprogramming non-cancer stem cells (CSCs) into PCSCs [5,6]. Consequently, PCSCs play a pivotal role in driving drug resistance and disease progression.

MicroRNAs (miRNAs), ~22-nucleotide (nt) non-protein-coding RNAs, are important posttranscriptional regulators of gene expression. MicroRNA-34a (miR-34a) is a bona fide tumor suppressor, which is downregulated in a wide range of solid tumors and hematological malignancies [7,8]. Of significance, miR-34a functions as a potent CSC suppressor by targeting key molecules essential for the survival and activities of CSCs [5,7]. In fact, extensive studies have shown that miR-34a exhibits anti-PCSC effects by targeting invasiveness and metastasis [9–11], stemness [12,13], epigenome [14,15], and cell survival [13,15,16]. Our earlier data revealed that systemic delivery of miR-34a reduced prostate tumor burden and lung metastasis by inhibiting PCSCs via targeting CD44 [11]. This indicates that miR-34a is a promising therapeutic for PCSC-enriched advanced PCa.

Despite extensive translational research in the field, the development of miR-34a therapeutics has been hampered by several challenges including delivery vehicle-associated toxicity, inadequate cellular uptake and stability, and limited specificity in targeted delivery to tumors [17,18]. Current delivery strategies for miR-34a therapeutics fall into two general categories: packaged vehicles such as liposomes and nanoparticles, and vehicle-free delivery such as ligand conjugates [5,19]. Major challenges of packaged vehicles include immunogenic effects and toxicities due to off-target effects associated with non-specific delivery [20]. To overcome these barriers, the ligand conjugation approach has been explored to achieve specific delivery of miR-34a to cancer cells, thereby enhancing therapeutic efficacy while minimizing toxicity. The concept is to directly conjugate a targeting ligand to miR-34a without a delivery vehicle. Typically, these targeting ligands are small molecules that exhibit both high affinity and specificity for receptors. On the other hand, the target receptors should be overexpressed on the surface of cancer cells relative to normal cells, and their expression level should be sufficient to enable the delivery of therapeutic quantities to tumor cells. A successful example is developing folate-conjugated miR-34a (folate-miR-34a) to target breast and lung cancers via folate receptor  $\alpha$  (FOLR1) [21]. Folate is an essential vitamin and a high-affinity ligand for the FOLR1, which is highly upregulated in ovarian, lung, breast, and other cancers [22]. Orellana et al. were the first to design and synthesize folate-miR-34a and showed that folate-miR-34a was selectively targeted to FOLR1-expressing tumors, downregulated target genes, and suppressed the tumor growth *in vivo* in lung and breast cancers [21]. Interestingly, folate can also bind to another membrane, the protein prostate-specific membrane antigen (PSMA), which is a clinically validated therapeutic target for PCa. PSMA is highly upregulated in PCa, and its expression has been associated with PCa progression [23–25].  $^{177}\text{Lu}$ -PSMA-617 (Pluvicto<sup>TM</sup>), which combines a PSMA-specific peptidomimetic with a therapeutic radionuclide, was the first FDA-approved PSMA-targeting therapy for metastatic PCa patients in 2022. Currently, there are several PSMA-targeting therapies undergoing clinical development, which include antibody-drug conjugates, PSMA-targeting immunotherapies, radioligand therapy, and photodynamic therapy [25,26]. With these considerations, we hypothesized that folate-miR-34a can be a potential therapeutic for treating PCa by targeting PCa cells expressing FOLR1 and/or PSMA.

In this study, we first show that miR-34a, a p53 transcriptional target, is significantly downregulated in PCa that have sustained p53 loss or mutations. We then show that folate-miR-34a, unexpectedly, did not elicit PCa-inhibitory effects, even in PSMA-expressing PCa cells. Further studies revealed that FOLR1, the major receptor for folate, is barely expressed in PCa. While our findings expose challenges associated with achieving

the specific delivery of folate–miR-34a to PCa, we provide evidence that folate–miR-34a may be a therapeutic agent for FOLR1-expressing cancers including ovarian and cervical cancers. Importantly, the insights obtained from the current study shed light on the future development of ligand-conjugated (and unconjugated) miR-34a as potential therapeutics for advanced and aggressive PCa.

## 2. Results

### 2.1. miR-34a Expression Is Downregulated in PCa That Has TP53 Loss or Mutations

miR-34a is known to be a p53-regulated miRNA and a crucial component of the p53 tumor suppressor network [27–29]. Previously, we provided preliminary data showing that the expression levels of both mature miR-34a and pre-miR-34a (Figure 1A) are significantly reduced in TP53-mutated compared to TP53 WT prostate tumors [5]. This suggests a reciprocal association between TP53 status and miR-34a levels in PCa. Herein, we further distilled TP53 genetic alterations utilizing the TCGA (Cancer Genome Atlas) database and found that approximately 46% of primary PCa patients exhibit TP53 alterations, including loss of heterozygosity (29%), mutations (12.2%), homozygous deletion (homodeletion; 4%), and fusion (1.2%) (Figure 1B). Among the mutations, missense mutations make up 8%, followed by 3% truncation mutations, and 1.2% splice mutations (Figure 1B). Notably, we observed a significant decrease in the levels of both pre-miR-34a and mature miR-34a in TP53-altered tumors (Figure 1C,D). Detailed dissection of TP53 genetic alterations revealed that downregulated miR-34a expression was contributed, primarily, by heterozygous loss and missense and truncation mutations but not homodeletion (Figure 1E,F). These results, collectively, indicate that miR-34a expression is significantly reduced in PCa with TP53 abnormalities and suggest that miR-34a-based therapeutics may be particularly effective in TP53-mutated prostate tumors.

### 2.2. miR-34a Mimic Downregulated miR-34a Targets and Inhibited PCa Cell Growth

We employed RT-qPCR to determine the expression levels of miR-34a-5p in four pairs of androgen-dependent (AD) and androgen-independent (AI) human PCa xenografts (LAPC9, LNCaP, LAPC4, and VCaP), four cultured PCa cell lines (LNCaP, VCaP, PC3, and DU145), and one immortalized but non-transformed prostate epithelial cell line (RWPE-1). The results revealed that miR-34a was heterogeneously expressed across xenografts and cell lines (Figure 2A). Compared to cultured RWPE-1 cells with WT TP53, the four cultured PCa cell lines showed decreased miR-34a expression (Figure 2A). Notably, miR-34a was further underexpressed in TP53-altered PCa cell lines (VCaP, DU145, and PC3) compared to LNCaP cells with WT TP53 (Figure 2A). A similar trend was found in PCa xenografts where the miR-34a levels were lower in TP53-mutated LAPC4 and VCaP xenografts as opposed to TP53 WT LAPC9 and LNCaP xenografts (Figure 2A). These results are consistent with the above bioinformatics analysis showing that miR-34a expression correlates with TP53 status (Figure 1).

PC3 is the most aggressive PCa cell line, being TP53 null and AR negative and having the lowest level of miR-34a (Figure 2A). We transfected miR-34a mimic to PC3 cells using lipofectamine RNAiMax, which led to significantly increased levels of miR-34a-5p compared to PC3 cells transfected with the negative control (NC) non-targeting oligonucleotides (Figure 2B). miR-34a significantly reduced Renilla luciferase activity in PC3-miR-34a sensor cells (Figure 2C), which are PC3 cells that stably express an miR-34a Renilla luciferase (Renilla) sensor [21]. The sensor includes an miR-34a complementary sequence downstream of the Renilla luciferase gene, allowing for monitoring the targeted silencing mediated by exogenous miR-34a. Transfected miR-34a also significantly downregulated the mRNA levels of miR-34a target genes *CD44*, *Cyclin D1*, *Myc*, and *BCL-2* (Figure 2D), and protein levels of CD44, Cyclin D1, and c-Myc in a dose-dependent manner (Figure 2E,F). Notably, miR-34a inhibited PC3 cell growth (Figure 2G).

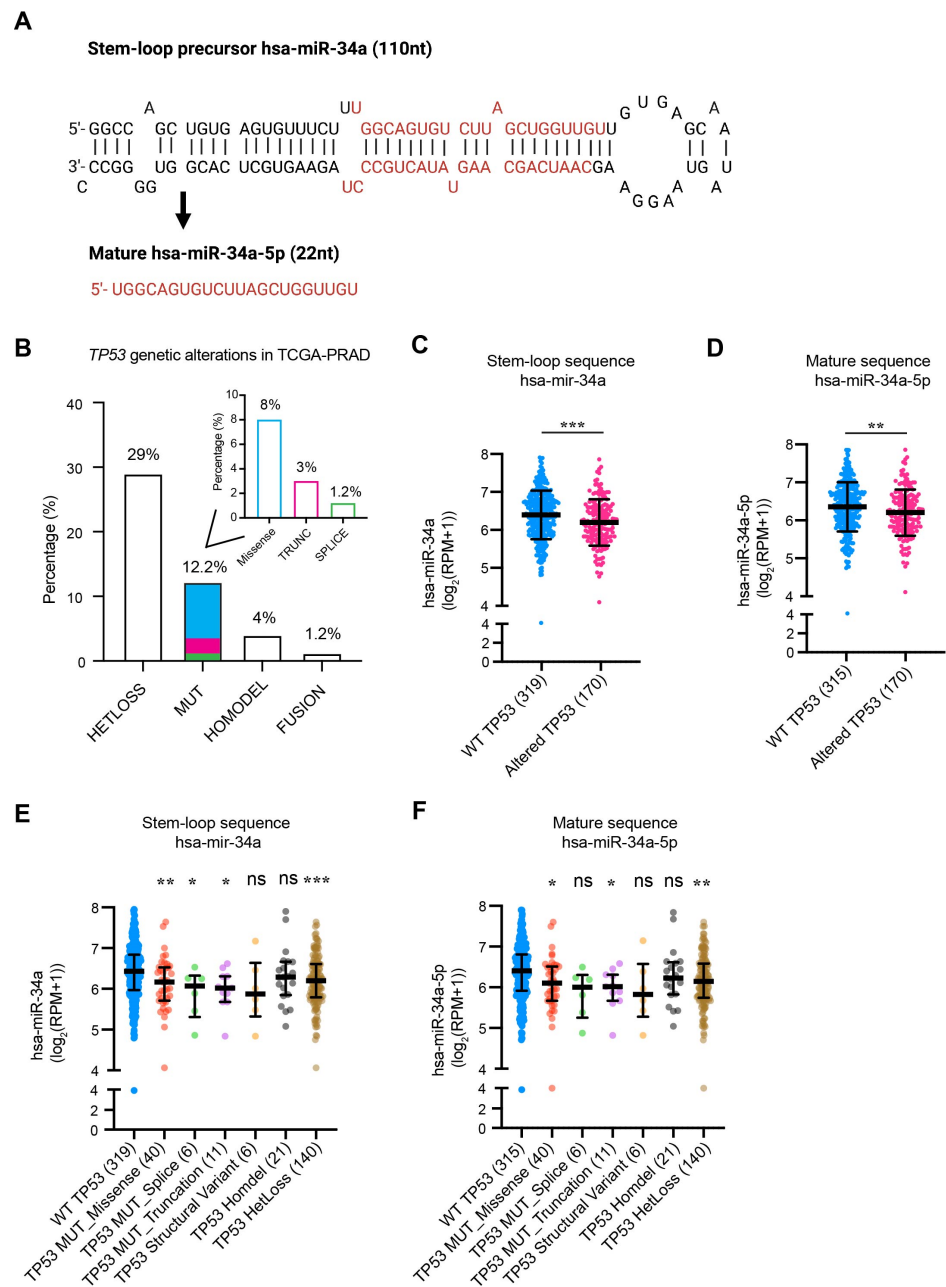


**Figure 1.** The structure of miR-34a and its regulation by TP53. (A) Schema of miR-34a structure (stem-loop precursor and mature strand). (B) The frequency of TP53 genetic alterations in PCa. The inset bar graph shows the detailed types of TP53 mutations (MUT) including missense, truncation (TRUNC), and splice mutations. HETLoss, heterozygous loss; HOMODEL, homozygous deletion. (C,D) Stem-loop (C) and mature (D) miR-34a expression in PCa patients with wild-type (WT) or altered TP53. (E,F) Stem-loop (E) and mature (F) miR-34a expression in PCa based on TP53 genetic alterations. All data were retrieved from Xena Browser and cBioPortal TCGA-PRAD. \*,  $p < 0.05$ ; \*\*,  $p < 0.01$ ; \*\*\*,  $p < 0.001$ ; ns, not significant (Student's  $t$ -test, as compared to WT).

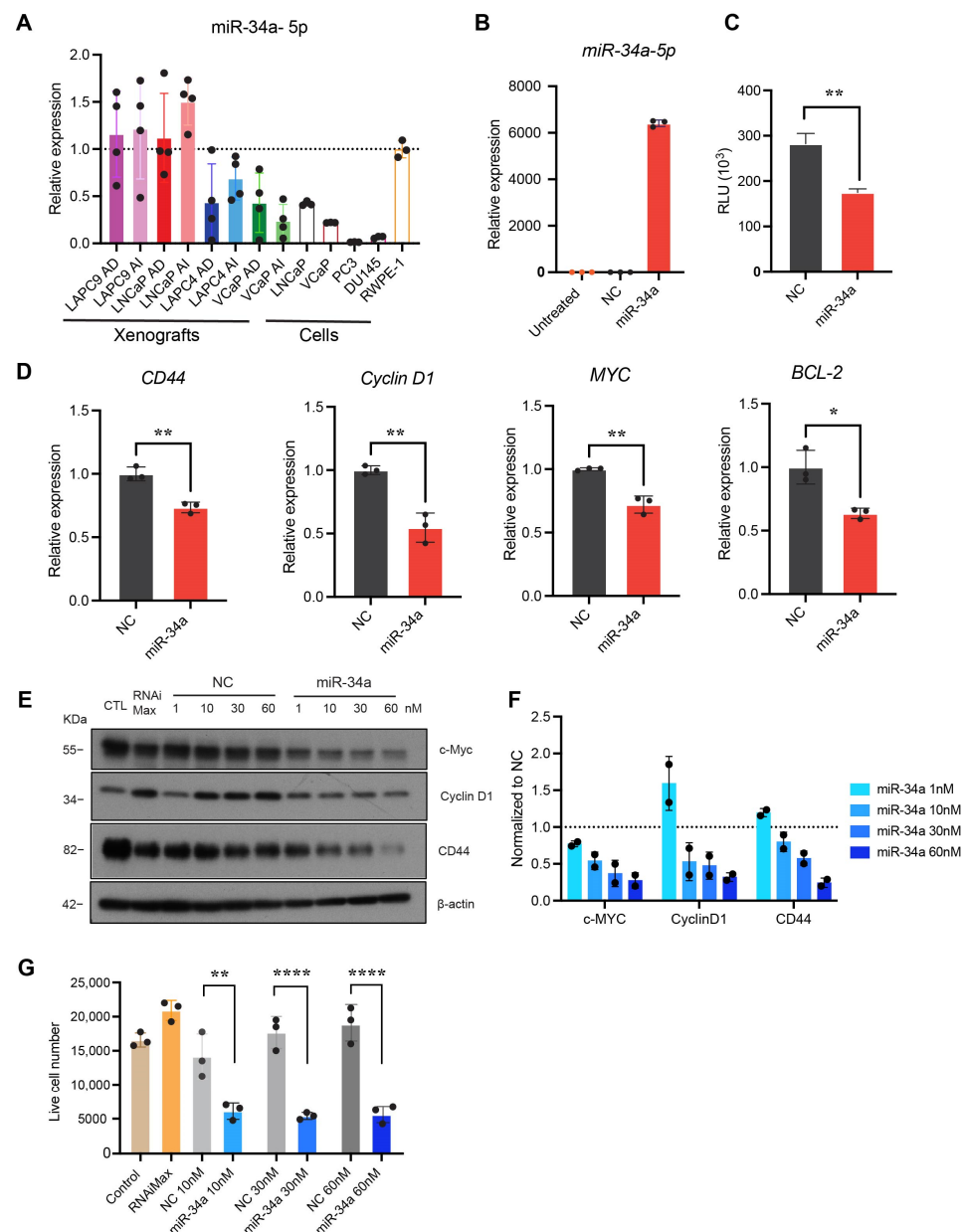


**Figure 2.** miR-34a expression in PCa cells and xenografts and miR-34a mimic downregulated molecular targets and inhibited PCa cell growth. (A) miR-34a-5p expression levels in four pairs of PCa xenografts and indicated PCa cell lines. AD, androgen-dependent; AI, androgen-independent. (B) miR-34a-5p expression 48 h post-transfection of PC3 cells with 30 nM miR-34a mimic or NC ( $n = 3$ ). (C) Targeted silencing of miR-34a Renilla sensor using miR-34a mimic in PC3-miR-34a sensor cells in vitro. Data points were normalized to NC ( $n = 3$ ). (D) Evaluation of the expression of miR-34a targets by qRT-PCR from PC3 cells following transfection with 30 nM miR-34a mimic for 48 h. (E) Representative Western blot images depicting downregulation of c-Myc, Cyclin D1, or CD44 expression following transfection of PC3 cells with miR-34a ( $n = 3$ ). (F) Quantitative data from E normalized to respective NC. (G) Effect of miR-34a mimic on PC3 cell growth measured by trypan blue cell counting 120 h after transfection of the indicated conditions. ( $n = 3$ ). In all experiments, miR-34a mimic or NC were transfected into PC3 cells using lipofectamine RNAiMax. \*,  $p < 0.05$ ; \*\*,  $p < 0.01$ ; \*\*\*,  $p < 0.0001$  compared to respective NC.

### 2.3. Folate-miR-34a Inhibited the Growth of Breast, Ovarian, and Cervical but Not PCa Cells

Next, we explored the potential “therapeutic” effects of folate-conjugated miR-34a, i.e., folate-miR-34a duplex, in PCa cells (Figure 3). Both miR-34a-3p passenger strand and

miR-34a-5p active strand underwent partial chemical modifications with 2'-O-methyl RNA bases (Figure 3A), and folate-miR-34a was synthesized by conjugating folate to miR-34a-3p passenger strands using click chemistry followed by an annealing step (Figure 3B). Finally, folate-miR-34a conjugates were evaluated using polyacrylamide gel electrophoresis (Figure 3C). As a previous study has shown that folate-miR-34a is selectively targeted to breast and lung cancers overexpressing FOLR1 [21], we first confirmed the functionality of our folate-miR-34a using the MDA-MB-231 breast cancer cells as the experimental control. MDA-MB-231-miR-34a and LNCaP-miR-34a "sensor" cells were established by stably expressing an miR-34a complementary sequence downstream of the Renilla luciferase gene [21]. As expected, the unconjugated miR-34a duplex without transfection reagent did not show any effect in either MDA-MB-231-miR-34a or LNCaP-miR-34a sensor cells (Figure 3D,E). Seventy-two hours post-transfection, folate-miR-34a significantly down-regulated Renilla luciferase activity in MDA-MB-231-miR-34a sensor cells (Figure 3D) but, surprisingly, not LNCaP-miR-34a sensor cells (Figure 3E). Also, folate-miR-34a, at 200 nM, inhibited the growth of MDA-MB-231 (Figures 3F and S1A), Hela (cervical cancer) (Figures 3G and S1B), and OV90 (ovarian cancer) (Figures 3H and S1C) cells but not that of LNCaP and PC3 PCa cells (Figures 3I,J and S1D,E) although folate-miR-34a transfected by lipofectamine RNAiMax significantly repressed the growth of all five cell lines at 50 nM (Figures 3F–J and S1A–E). Collectively, these results indicate that folate-miR-34a, as expected, inhibited the growth of FOLR1-expressing breast, cervical, and ovarian cancer cells but, unexpectedly, did not exhibit any inhibitory effects on PCa cells.

#### 2.4. Lack of FOLR1 Expression in PCa

The above results suggest that PCa cells might express little or no FOLR1. To test this possibility, we first investigated, via bioinformatics approaches, *FOLR1* mRNA levels in the normal prostate and PCa in vivo. The GTEx data show that among normal tissues, the levels of *FOLR1* mRNA are high in the lung, salivary gland, kidney, and thyroid gland but very low in the normal prostate (Figure S2A). We then evaluated *FOLR1* mRNA expression across 33 human cancers, paired normal tissues in TCGA, and combined the results in benign/normal tissues in GEPIA (Gene Expression Profiling Interactive Analysis, <http://gepia.cancer-pku.cn/>) database (Figure 4). We found that *FOLR1* mRNA was indeed very lowly expressed in both normal prostatic tissues and prostate tumors (PRAD) although its expression levels were high and elevated in several cancers including ovarian cancer (OV), glioblastoma (GBM), pancreatic adenocarcinoma (PAAD), rectum adenocarcinoma (READ), testicular germ cell tumor (TGCT), uterine corpus endometrial carcinoma (UCEC), and uterine carcinosarcoma (UCS) (Figure 4). On the contrary, the *FOLR1* mRNA levels were decreased in six cancers including breast cancer (BRCA), lung squamous cell carcinoma (LUSC), head and neck squamous cell carcinoma (HNSC), kidney chromophobe (KICH), acute myeloid leukemia (LAML), and skin cutaneous melanoma (SKCM) (Figure 4). Interestingly, the *FOLR1* mRNA levels, although low, were also reduced in PCa compared to normal prostate (Figure S2B). Intriguingly, the low levels of *FOLR1* mRNA were detected preferentially in AR<sup>+</sup> luminal epithelial cells in normal human prostate (Figure S2C) based on our RNA-seq analysis using purified cell populations [30]. Also, the low *FOLR1* mRNA levels showed an increased tendency in two PCa patient cohorts [31,32] who went through short-term neoadjuvant androgen deprivation therapy (ADT) (Figure S2D,E).

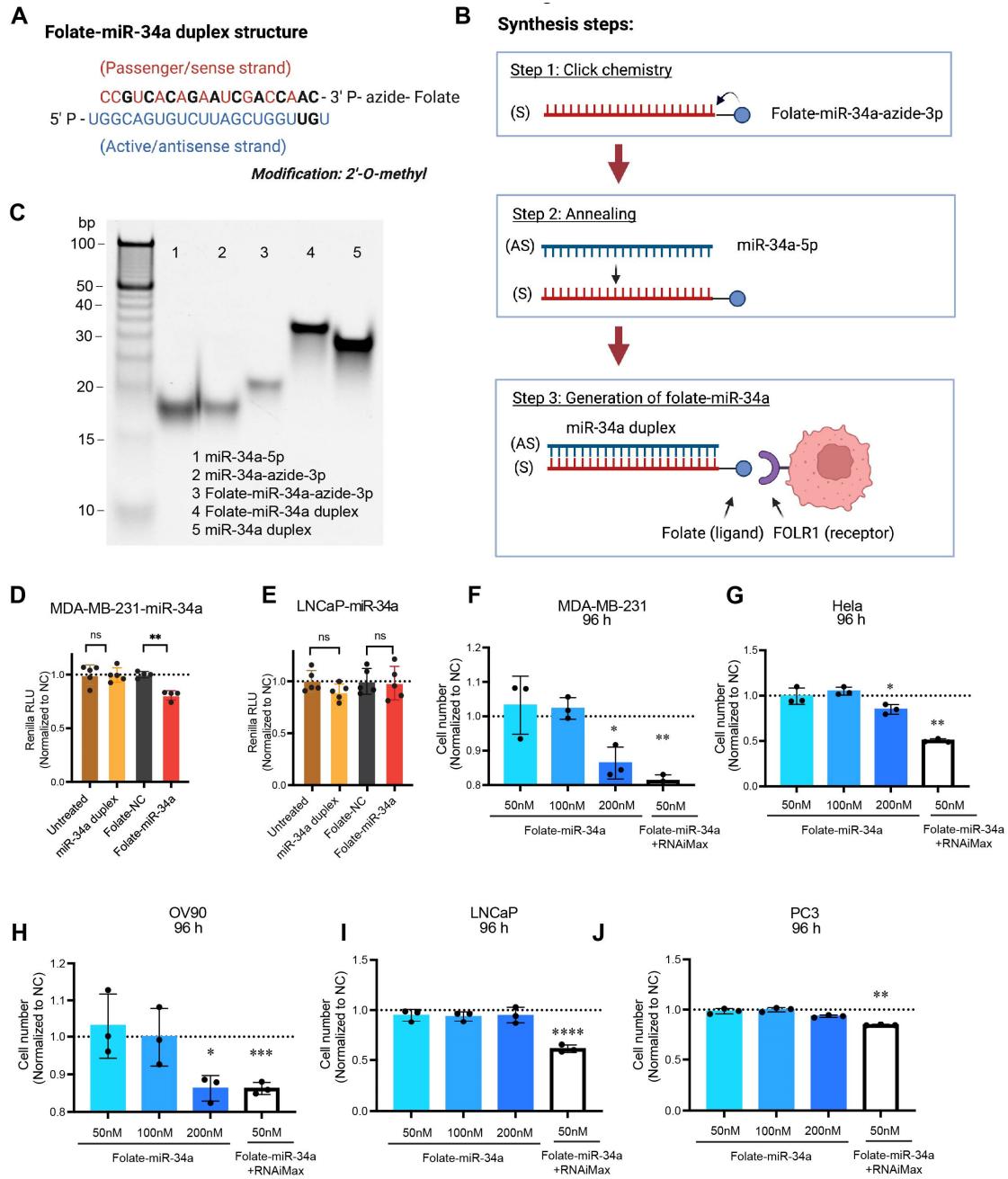


**Figure 3.** Synthesis of folate-miR-34a and its biological effects in four different cancer cells. (A) The structure of folate-miR-34a duplex. Chemically modified nucleotides were marked in black. (B) The schema of folate-miR-34a synthesis process. S, sense strand; AS, antisense strand. (C) Evaluation of folate-miR-34a conjugation measured by 15% native TAE PAGE. (D,E) Targeted silencing of miR-34a Renilla sensor by folate-miR-34a in MDA-MB-231-miR-34a sensor cells (D) and LNCaP-miR-34a sensor cells (E). The results (RLU, relative luciferase unit) were normalized to folate-NC (negative control: scrambled miRNA) ( $n = 4$ ). (F-J) Effect of folate-miR-34a on proliferation in MDA-MB-231 (breast cancer), HeLa (cervical cancer), OV90 (ovarian cancer), LNCaP, or PC3 cells ( $n = 3$ ). \*,  $p < 0.05$ ; \*\*,  $p < 0.01$ ; \*\*\*,  $p < 0.001$ ; \*\*\*\*,  $p < 0.0001$  compared to respective NC.

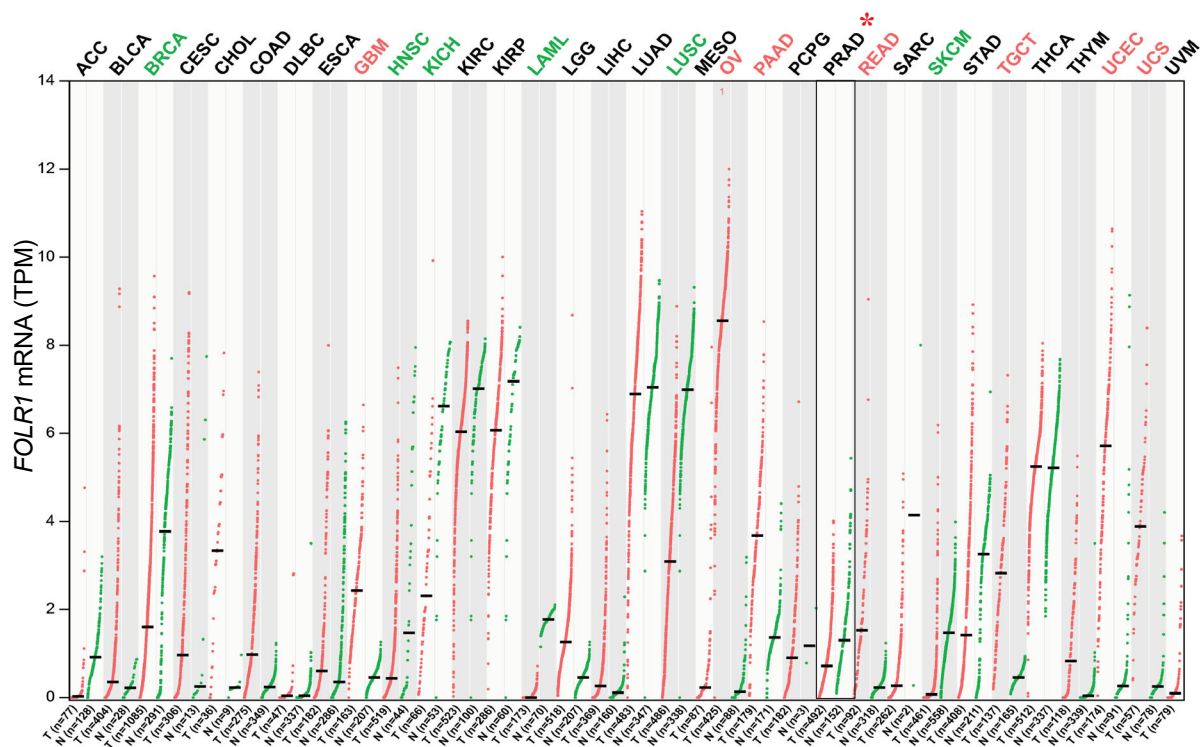


**Figure 4.** FOLR1 mRNA expression across 33 human tumors (T) and matched normal tissues (N). Significant increase or decrease in T compared to N is highlighted in red or green, respectively. Prostate cancer (PRAD) is marked with asterisk (\*).

Next, we investigated the expression of FOLR1 mRNA and protein levels in PCa cell lines and xenografts (Figure 5). In CCLE (Cancer Cell Line Encyclopedia), FOLR1 mRNA was barely expressed in PCa cell lines in contrast to ovarian, endometrial, and kidney cancer cells that highly expressed FOLR1 mRNA (Figures S2F and 5A). Our RT-qPCR (reverse transcription–quantitative polymerase chain reaction) and Western blotting also revealed FOLR1 to be barely expressed in PCa cells as well as prostate xenograft tumors at both mRNA and protein levels (Figure 5B,C). We also assessed the FOLR1 expression in PC3, LNCaP, and HeLa (positive control) cells using immunofluorescence (Figure 5D) and flow cytometry (Figure 5E–G), both of which showed that PC3 and LNCaP cells did not express FOLR1. To further visualize folate uptake in vitro and in vivo, we conjugated a near-infrared (NIR) dye to folate (i.e., folate–NIR). As shown in Figure 5H–J, in contrast to HeLa cells, LNCaP and PC3 PCa cells did not show any folate–NIR uptake in the cells.

### 2.5. Folate–miR-34a Also Did Not Accumulate Nor Show Any Effect in PSMA-Expressing PCa Cells

The above results indicate that folate–miR-34a may not be an effective PCa-targeting therapeutic due to a lack of appreciable FOLR1 expression. Folate (folic acid) has been reported to bind to another molecule, the prostate-specific membrane antigen (PSMA) [33,34]. PSMA, also known as glutamate carboxypeptidase II, is a type II membrane protein that is highly expressed in PCa [35]. PSMA is constitutively internalized and rapidly recycles back to the cell surface enabling additional rounds of internalization [19,36,37]. Yao et al. reported that PSMA can bind to folate at pH 7.4 and functions as a folate transporter and that PSMA expression significantly increased cellular uptake of folic acid under conditions of limiting folate in PCa cells [34]. Moreover, folate was able to compete with other substrates and inhibit the enzymatic activity of PSMA [34], indicating the folate-binding capability of PSMA. These studies suggest that folate–miR-34a might be able to gain access to PSMA-expressing PCa cells.



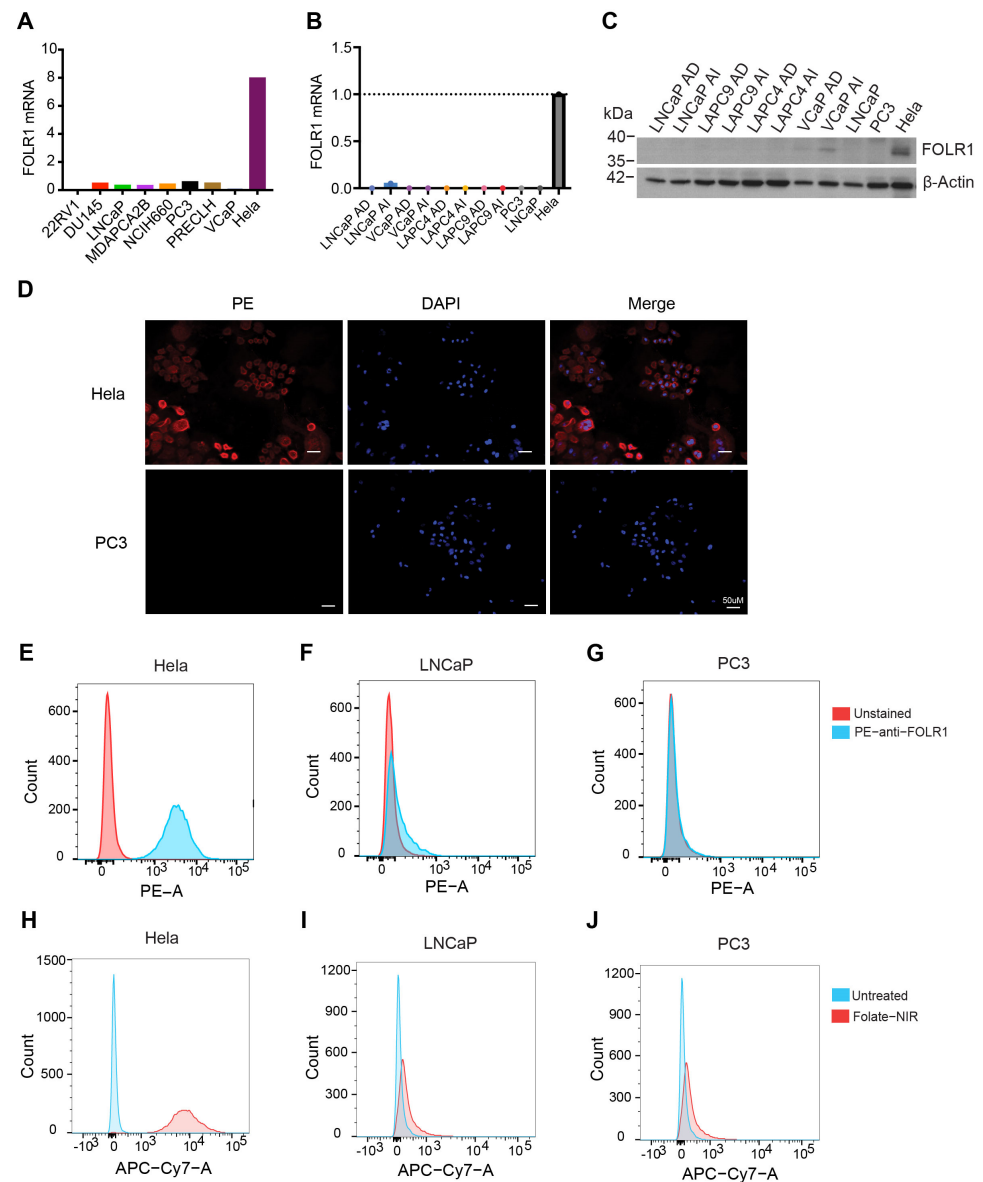


**Figure 5.** FOLR1 expression in PCa. (A) FOLR1 expression in PCa cell lines in the Cancer Cell Line Encyclopedia (CCLE). (B,C) The mRNA (B) and protein (C) levels of FOLR1 in four pairs of PCa xenografts and cell lines. (D) Representative immunofluorescent images showing the expression of FOLR1 (PE) in HeLa cells but not in PC3 cells. (E–G) Flow cytometry analysis (using PE-conjugated anti-FOLR1 antibody) showing expression of FOLR1 in HeLa (E) but not in LNCaP (F) or PC3 (G) cells. (H–J) Folate–NIR uptake in FOLR1<sup>+</sup> HeLa cells (H) compared to FOLR1<sup>−</sup> LNCaP (I) and PC3 (J) cells. Histograms represent overlaid flow cytometry data of unstained cells and cells stained with folate–NIR (50 nM). Flow cytometry was analyzed on Cy7 channel.

Unfortunately, we did not observe any biological effects of folate–miR-34a on PSMA-expressing LNCaP cells (Figures 3E,I and S1D) nor did we observe folate–NIR uptake in LNCaP cells (Figure 5I). In addition, fluorescence microscopy studies revealed prominent folate–NIR accumulation in FOLR1-expressing HeLa cells but not in PC3 cells, which do not express FOLR1 or PSMA nor in LNCaP cells, which lack FOLR1 but do express PSMA [38] (Figure 6A–C). We also conducted in vivo biodistribution studies of folate–NIR to monitor its targeting specificity in PCa xenografts, and the results revealed that 24 h after injection, folate–NIR was not retained in LNCaP AD/AI or LAPC9 AD/AI tumor tissues but cleared mainly by the kidney of the host mice (Figure 6D–G), whereas it was significantly accumulated in HeLa tumor tissues (Figure 6H). Analysis of the tumor/kidney

ratio further supported the limited accumulation of folate–NIR in prostate tumors as compared to HeLa tumors that highly express FOLR1 (Figure 6I).

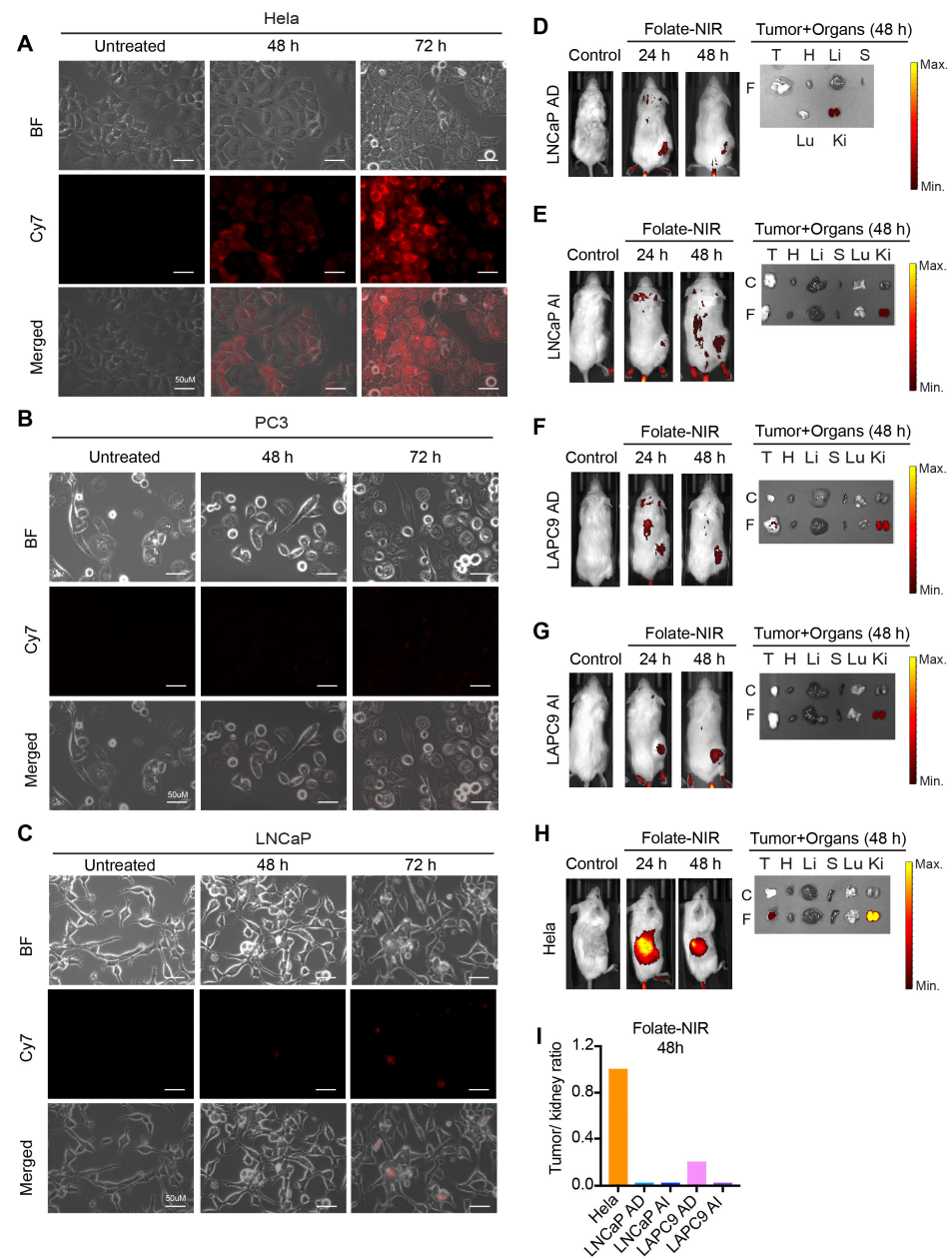


**Figure 6.** In vitro cellular uptake and in vivo biodistribution of folate–NIR in PCa. (A–C) Immunofluorescence analysis of folate–NIR uptake in FOLR1<sup>+</sup>PSMA<sup>−</sup> HeLa cells (A) compared to FOLR1<sup>−</sup>PSMA<sup>−</sup> PC3 (B) and FOLR1<sup>−</sup>PSMA<sup>+</sup> LNCaP (C) cells. Scale bars, 50  $\mu$ m. Folate–NIR was analyzed using Cy7 filter. (D–H) Left: representative live imaging of mice bearing the indicated LNCaP AD/AI, LAPC9 AD/AI, or HeLa xenograft tumors after intravenous injection of a single dose (10 nmol) of folate–NIR and analyzed at indicated time points (control, time 0). Right: *ex vivo* tissue biodistribution in mice 48 h after administering folate–NIR (T, tumor; H, heart; Li, liver; S, spleen; Lu, lungs; Ki, kidneys). (I) The tumor/kidney ratio determining folate–NIR retention in xenograft tumors quantified from (D–H).

Collectively, these data suggest that folate is not a suitable ligand for targeting miR-34a efficiently in PCa cells.

### 3. Discussion

Many studies have demonstrated that miR-34a represents a promising anti-CSC inhibitor for treating advanced PCa [5,7,11]. However, the lack of efficient and safe delivery strategies remains a major bottleneck in clinical failure, largely due to the systemic toxicity caused by the packaging vehicle and the immunotoxicity likely associated with miR-34a over-dosing [7,39,40]. In this study, we attempted to develop a package-free targeted delivery platform, i.e., folate–miR-34a, for PCa therapy. Unfortunately, folate–miR-34a did not exhibit appreciable uptake in PCa cells and did not elicit any PCa-inhibitory effects due to the lack of expression of FOLR1, the major high-affinity receptor of folate, in PCa cells. Folate–miR-34a did not even show any uptake and biological effects in PCa cells that express PSMA, which can bind folate (as an enzymatic substrate) and function as a folate transporter [34,41]. In PC3 cells that do not express endogenous PSMA, PSMA re-expression significantly increased cellular uptake of folic acid under conditions of limiting folate [34]. Also, folate was able to compete with other substrates and inhibited the enzymatic activity of PSMA [34], further supporting the folate-binding capability of PSMA. Furthermore, previous studies reported that folate-conjugated delivery platforms could achieve specific delivery of various payloads to PSMA-expressing PCa cells and demonstrated better anti-cancer efficacy *in vivo* as compared to non-targeted ones [38,42–45]. These early studies [34,38,41–45] provide the rationale for the targeted delivery of folate-conjugated miR-34a to PSMA-expressing PCa. However, our data herein show that folate–miR-34a was not uptaken by and did not achieve specific delivery to PSMA<sup>+</sup> LNCaP cells. These “inconsistent” results may likely be related to different chemistries of folate–drug conjugates, and a significant difference is that all previous studies conjugated folate to liposomes, nanocarriers, or bacterial minicells. Since the payloads are encapsulated in those vehicles, drugs may become internalized into the PCa cells through endocytosis, and the observed therapeutic effects, in principle, could be due to off-target (i.e., PSMA-independent) effects. Another consideration is that the binding affinities for folate to FOLR1 and PSMA are different. The affinity of folate for PSMA is much lower than FOLR1 [19], which could result in less miR-34a being delivered. Also, very little miR-34a was released from the endosome due to endosome entrapping. These two limitations could together lead to the minimal therapeutic effect of folate–miR-34a on PSMA-expressing PCa cells. On the other hand, folate–miR-34a inhibited cell proliferation in breast, cervical, and ovarian cancer cells that highly express FOLR1, indicating its potential therapeutic applications for these FOLR1-expressing cancers. FOLR1 has been associated with tumor relapse and chemotherapy resistance in cervical and ovarian cancers [46,47]. FOLR1 has emerged as an optimal target and multiple FOLR1 targeting therapeutic approaches have been or are being tested preclinically and clinically [48–52]. In-depth preclinical studies of folate–miR-34a are needed to validate the efficacy and safety in cervical and ovarian cancers.

PSMA is highly expressed in metastatic CRPC and has been shown to be a validated therapeutic target. Currently, ARX517, an antibody–drug conjugate composed of a fully humanized anti-PSMA mAb linked to AS269 as a potent microtubule inhibitor, is being studied in phase I/II clinical trials enrolling patients with metastatic CRPC. DUPA is a synthetic urea-based ligand that can bind to PSMA with high affinity, leading to saturation of the receptor in a short period of time [23]. Thomas et al. were the first to use DUPA conjugates to deliver siRNAs selectively to PSMA-expressing PCa cells [53]. Treating LNCaP cells with fluorescently tagged siRNA directly linked to DUPA (DUPA-siRNA-cy5) *in vitro* resulted in substantial uptake within 1 h of treatment [48]. Similarly, a significant accumulation of DUPA-siRNA was observed in LNCaP xenograft tumors after intravenous injection of DUPA-siRNA-cy5. Another study by Tai et al. showed that DUPA-siRNA induced tumor growth inhibition in LNCaP xenografts [54]. These studies suggest that DUPA-conjugated miR-34a could be a potential therapeutic to target PSMA-expressing PCa. Considering the huge success of lipid nanoparticle (LNP) application in COVID-19 vaccines, DUPA-conjugated LNP with miR-34a as the payload could be another novel delivery approach to explore in the future.

Ligand-directed miR-34a delivery potentially represents a novel strategy to achieve specific and efficient delivery for targeting a wide range of cancer types. In comparison to packaged vehicles, this strategy circumvents off-target effects and non-specific biodistribution that result in systematic toxicity. Nevertheless, there are still many obstacles to overcome in translating the ligand-directed miR-34a as PCa-targeting therapeutics (Figure 7). For example, PCa lacks appreciable FOLR1 expression invalidating folate–miR-34a as a therapeutic in this cancer (Figure 7A). Another concern is endosomal entrapment of ligand-conjugated miR-34a (Figure 7B), which, in fact, represents the major challenge for ligand-conjugated miRNA delivery. Once ligand-conjugated miR-34a is internalized in PCa cells, miR-34a must successfully escape from the endosome into the cytoplasm, where it can interact with the RNAi machinery. Otherwise, it will be subject to lysosomal degradation when the late endosomes fuse with the lysosomes. Various strategies have been developed to promote endosomal release including cell-penetrating peptides, fusogenic and endolytic peptides, or chemical agents such as chloroquine and nigericin [55–59]. Some of these approaches are limited in translation due to systematic toxicity *in vivo*, and more efforts are needed to develop effective and less toxic endosomal agents aiming to further enhance the efficacy of ligand-conjugated miR-34a therapeutics.

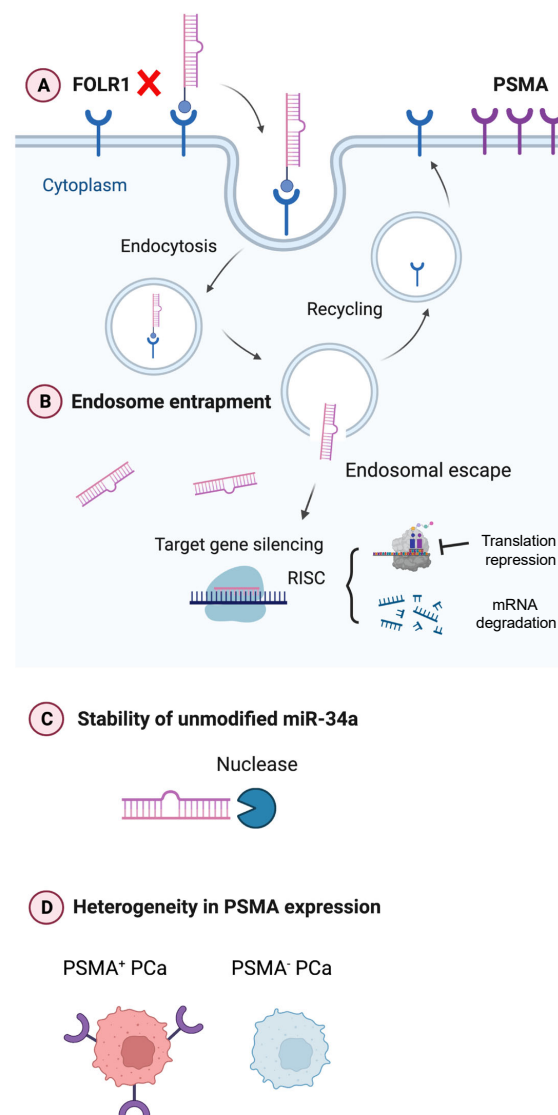


**Figure 7.** Graphical abstract. Current challenges in developing ligand-directed miR-34a therapeutics in PCa. See text for details.

Instability and (exo)nuclease-mediated degradation of unmodified miR-34a presents another issue (Figure 7C). Chemical modifications of miRNAs, including the introduction of 2'-O-methyl and 2'-fluoro to the ribose, and phosphorothioate substitutions to the backbone, have been used to improve serum stability and increase intracellular half-life to ultimately reduce the therapeutic doses [19,60]. The miR-34a used in the current study is a partially modified (PM) version containing a minimal number of 2'-O-methyl modifications akin to commercially available miR-34a mimics [21,61]. In preliminary studies, we observed that both PM miR-34a duplex and PM folate-miR-34a duplex started degradation from 10 min and nearly 50% of oligos were degraded within 30 min, demonstrating the instability of PM miR-34a oligos (Figure S3). This suggests that chemical modifications should be carefully designed and selected to improve the stability of miR-34a therapeutics. A very recent study by Abdelaal et al. demonstrated that full chemical modification of miR-34a duplex enhances both the stability and activity of miR-34a [61]. This improved stability could be beneficial for in vivo applications by reducing the effective dose as well as minimizing toxicity resulting from higher miRNA doses or administration frequency.

Finally, the heterogeneity in the expression levels of targets, i.e., cancer cell surface receptors (e.g., FOLR1) and membrane proteins (e.g., PSMA) should be considered as one of the limiting factors for ligand-directed miR-34a therapeutics (Figure 7D). *A priori*, PSMA represents an ideal target for PCa treatment due to its highly specific cell surface expression, which lends possibilities for both imaging and therapeutic development. However, PSMA expression exhibits significant intra- and inter-tumor heterogeneity in advanced PCa [62–64], as also highlighted by recent preclinical and clinical studies demonstrating that not all patients with PSMA-positive PCa respond to PSMA-targeted radionuclide  $^{177}\text{Lu}$ -PSMA-617 [65]. PSMA expression is known to be (partially) regulated by AR, and AR<sup>+</sup> PCa cells are generally PSMA<sup>+</sup> whereas AR<sup>-</sup> PCa cell lines are PSMA<sup>-</sup>. But interestingly, a subset of AR<sup>-</sup> CRPC and neuroendocrine PCa (NEPC) did express PSMA [62], indicating alternative mechanisms of PSMA regulation including, among others, transcriptional regulation by HOXB13 [62], deleterious DNA repair aberrations [63], and epigenetic silencing by CpG methylation [64]. Some pharmacological approaches can augment PSMA levels in PCa. For example, treatment with histone deacetylase (HDAC) inhibitors reversed the epigenetic suppression, leading to PSMA re-expression both in vitro and in vivo [64]. A deeper understanding of the biology of PSMA in PCa is needed to elucidate pharmacological strategies that can help tackle the heterogeneity in PSMA expression (Figure 7D) and thus enhance the efficacy of PSMA-targeted therapies for advanced PCa.

## 4. Materials and Methods

### 4.1. Cell Lines and Animals

LNCAp, PC3, DU145, VCaP, and RWPE-1 cells were purchased from the American Type Culture Collection (ATCC). MDA-MB-231-miR-34a reporter cells and LNCAp-miR-34a sensor cells were kind gifts from Dr. Andrea Kasinski (Purdue University). PC3-miR-34a sensor cells were generated as described previously [21]. MDA-MB-231, OV90, and Hela cells were gifts from Drs. Chetan Oturkar and Shamshad Alam (Roswell Park Comprehensive Cancer Center). VCaP cells were cultured in DMEM medium supplemented with 10% fetal bovine serum (FBS) and antibiotics. RWPE-1 were cultured in Keratinocyte Serum Free Medium (K-SFM) supplemented with 0.05 mg/mL bovine pituitary extract (BPE) and 5 ng/mL human recombinant epidermal growth factor (EGF). Except for VCaP and RWPE-1 cells, all other cell lines were cultured in RPMI medium plus 10% heat-inactivated fetal bovine serum (FBS) plus antibiotics. These cell lines were authenticated regularly in our institutional CCSG Cell Line Characterization Core and also examined to be free of mycoplasma contamination. LAPC4 and LAPC9 xenograft lines were initially provided by Dr. Robert Reiter (UCLA) and have been used extensively in our previous studies [4,11]. Immunodeficient mice, NOD/SCID (non-obese diabetic/severe combined immunodeficiency), and NOD/SCID-IL2R $\gamma$ <sup>-/-</sup> (NSG) were obtained from the Jackson Laboratory, and breeding colonies were maintained in standard conditions in our animal facilities.

#### 4.2. Preparation of Folate–miR-34a Duplex

miR-34a duplex was constructed using two RNA oligonucleotides: miR-34a-5p guide strand and miR-34a-3p passenger strand (Integrated DNA Technologies, Ann Arbor, MI, USA). A scrambled miRNA (negative control, NC) synthesized with the same modifications was used to form a control duplex. The synthesis of folate–miR-34a duplex was previously described [21]. In brief, a click reaction was conducted between folate–DBCO and azide-modified passenger miR-34a (or scramble). Click reaction was performed at a 1:10 molar ratio (azide oligo/folate–DBCO) at room temperature in water for 10 h and then cooled to 4 °C overnight. Unconjugated folate was removed from the reaction using Oligo Clean & Concentrator (Zymo Research, Irvine, CA, USA) per the manufacturer's instructions.

After conjugation, the miR-34a-5p guide strand was annealed to the folate–miR-34a-azide-3p passenger strand at an equal molar ratio in the presence of annealing buffer (10 mM Tris buffer, pH 7 (Sigma, St. Louis, MO, USA), 1 mM EDTA (Sigma), 50 mM NaCl (Sigma)) followed by incubation at 95 °C for 5 min, and slow cooling to room temperature for 1.5 h. Annealed oligos were then stored at –80 °C. Conjugation was verified using 15% tris base, acetic acid, and EDTA (TAE) native PAGE.

#### 4.3. RNA Isolation and Real-Time RT-PCR Analysis

Total RNA was extracted using Direct-zol RNA Miniprep Plus Kits (Zymo Research) according to the manufacturer's instructions. RNA concentration was quantified using a nanodrop. qRT-PCR was performed using a CFX Connect Real-Time PCR Detection System (Bio-Rad, Hercules, CA, USA). For miR-34a-5p expression assay, qPCR data were normalized to U6. For miR-34a target genes, qPCR data were normalized to GAPDH. Data were then analyzed using the  $2^{-\Delta\Delta Ct}$  method and expressed as fold change.

#### 4.4. In Vitro Renilla Luciferase Assay

MDA-MB-231-miR-34a reporter cells or LNCaP-miR-34a sensor cells were treated with 100 nM miR-34a duplex, 100 nM folate-NC, and 100 nM folate–miR-34a (hereafter referred to as folate-34a). At 72 h, Renilla-Glo Luciferase assay (Promega, Madison, WI, USA) was performed as per manufacturer instructions. In brief, Renilla-Glo Luciferase substrate was mixed with Renilla-Glo buffer at 1:1000 dilution followed by addition into each well. After shaking the plates at room temperature for 10 min, Renilla luciferase signal was measured using a BioTek Synergy microplate reader (Agilent, Santa Clara, CA, USA).

#### 4.5. Cell Proliferation Assays

For the functionality validation of miR-34a mimic (MC11030, Thermo Fisher, Waltham, MA, USA), PC3 cells were seeded onto individual wells of a 96-well plate. The next day, cells were transfected with miR-34a or NC at the indicated concentrations using Lipofectamine RNAiMAX (Life Technologies, Austin, TX, USA). At 96 h, trypan blue-excluding cells were counted with a hemocytometer and then compared to corresponding NC to determine relative cell growth. Similarly, for the evaluation of effects of folate–miR-34a in multiple cancer cell lines, cells were seeded onto individual wells of a 96-well plate. The next day, cells were treated with folate–miR-34a at the indicated concentrations or transfected with 50 nM folate–miR-34a using Lipofectamine RNAiMAX (Life Technologies). At the indicated time points, trypan blue-excluding cells were counted with a hemocytometer to determine relative cell growth by comparing them to corresponding NC.

#### 4.6. Western Blotting

For Western blotting analysis, whole cell lysate was prepared in RIPA buffer and run on 4–15% gradient SDS-PAGE gels. The proteins were transferred to nitrocellulose membrane followed by incubation with primary antibodies and corresponding secondary antibodies. Films were developed using Western Lighting ECL Plus reagent (PerkinElmer, Waltham, MA, USA). Antibodies used: c-Myc (E5Q6W) rabbit mAb (18583, Cell Signaling Technology, Danvers, MA, USA), Cyclin D1 (E3P5S) XP rabbit mAb (55506, Cell Signaling

Technology), CD44 (156-3C11) mouse mAb (3570, Cell Signaling Technology), and FOLR1 mouse mAb (sc-515521, Santa Cruz Biotechnology, Dallas, TX, USA).

#### 4.7. Immunofluorescence (IF)

Hela and PC3 cells were seeded onto 6-well plate, each containing a sterilized coverslip. On the next day, medium was aspirated and 1 mL of 4% formaldehyde was added to each well for 10 min. Coverslips were rinsed with 1X DPBS 3 times for 5 min each. Then cells were blocked with 5% BSA solutions at room temperature for 1 h. Then blocking solution was aspirated and the cells were incubated with phycoerythrin (PE) anti-FOLR1 antibody (908304, BioLegend, San Diego, CA, USA) at room temperature for 1 h. Coverslips were rinsed with 1X DPBS followed by mounting with ProLong Gold Antifade Reagent with DAPI (P36931, Thermo Fisher).

#### 4.8. Flow Cytometry

FOLR1<sup>+</sup> Hela cells, FOLR1<sup>-</sup> LNCaP cells, and FOLR1<sup>-</sup> PC3 cells grown in 10 cm culture dish were harvested (cell viability > 90%) and washed three times in ice-cold DPBS buffer supplemented with 0.5% BSA and aliquoted to a density of  $5 \times 10^6$  cells/mL in flow cytometry staining buffer (FC001, R&D Systems, Minneapolis, MN, USA). Next, flow cytometric analyses were performed following standard protocols. In brief,  $5 \times 10^5$ /100 $\mu$ L cells were incubated with Fc Receptor Binding Inhibitor Polyclonal Antibody (14-9161-73, eBioscience, San Diego, CA, USA) on ice for 20 min. Without washing, staining proceeded with primary antibody PE anti-FOLR1 antibody (908303, BioLegend) incubation followed by flow cytometric analysis using LSRFortessa flow cytometer (BD Biosciences, Franklin Lakes, NJ, USA). Data were analyzed using FlowJo software v10 (Tree Star Inc., Ashland, OR, USA). For the functionality of FOLR1, Hela cells, LNCaP cells, and PC3 cells were incubated with folate-NIR (50 nM) for the indicated time periods followed by flow cytometric analyses as described above.

#### 4.9. Fluorescence Microscopy

Hela cells, LNCaP cells, and PC3 cells were seeded into 6-well culture plate. Then spent medium was replaced with fresh medium containing folate-NIR (50 nM). At the indicated time points, fluorescence images were acquired using a KEYENCE BZ-X All-in-One Fluorescence Microscope.

#### 4.10. Whole Body Imaging and Tissue Biodistribution

Xenograft model: Briefly, all PCa AD (androgen-dependent) and AI (androgen-independent) xenograft tumors (LNCaP and LAPC9) were routinely maintained in intact immunodeficient NOD/SCID or NSG mice [4,11]. For the AI lines, parental AD tumor cells were purified, mixed with Matrigel, injected subcutaneously, and serially passaged in surgically castrated immunodeficient mice. For Hela xenograft tumors, Hela cells ( $2 \times 10^6$ ) were injected into the flank of 6–8-week-old female NOD/SCID mice. Once tumors reached approximately 300–400 mm<sup>3</sup> in volume, animals (2 mice/group) were intravenously injected with 10 nmol of folate-NIR in PBS. For vehicle control group, PBS was intravenously injected with PBS. Whole-body fluorescence images were acquired in mice at indicated time points using IVIS<sup>®</sup> Spectrum (Ex/Em = 745/800 nm). After whole-body imaging at the endpoint, animals were dissected and selected tissues were analyzed for fluorescence intensities using the IVIS<sup>®</sup> imager. The tumor-to-kidney ratio was calculated by dividing the average radiant efficiency of tumor by the average radiant efficiency of kidney for each xenograft.

#### 4.11. Statistical Analysis

Statistical analysis was performed using Prism statistical software version 10. Unpaired two-tailed Student's *t*-test was used to compare significance between two groups. One-way ANOVA was used to compare the differences among multiple groups and

multiple comparisons were corrected using Tukey's post hoc test. The results were presented as mean  $\pm$  S.D as denoted in the figure legends. Statistically significant  $p$ -values are as indicated in the corresponding figure legends.

## 5. Conclusions

- Folate-miR-34a did not elicit PCa-inhibitory effects due to a lack of appreciable expression of FOLR1 in PCa cells.
- Folate-miR-34a also did not display any apparent effect on PCa cells expressing PMSA despite folate's reported binding capability to PSMA.
- Folate-miR-34a exhibited impressive inhibitory effects on breast, ovarian, and cervical cancer cells that do express FOLR1, suggesting its potential therapeutic application on FOLR1-expressing cancers.
- The insights offered by the current study highlight challenges in the specific delivery of folate-miR-34a to PCa due to the lack of target receptor expression and shed light on the future development of ligand-conjugated miR-34a as potential therapeutics for advanced and aggressive PCa.

**Supplementary Materials:** The following supporting information can be downloaded at: <https://www.mdpi.com/article/10.3390/ijms25042123/s1>.

**Author Contributions:** W.L. conceived the project with D.G.T., designed and performed most experiments, interpreted the results, and wrote the manuscript draft. Y.W. provided partial bioinformatic data on FOLR1 and performed IF and some qPCR experiments. X.L. generated bioinformatics data on TP53. S.W. performed partial cell proliferation experiment. M.W. performed Western blotting experiment. S.G.T. and J.A.S. offered technical support on the IVIS imaging. A.T. maintained and provided human prostate cancer xenografts. A.M.A. and K.S. provided folate conjugates and key reagents. I.P., G.C. and A.L.K. discussed the content and critically reviewed the manuscript draft. D.G.T. aided in manuscript writing and finalized the manuscript. All authors have read and agreed to the published version of the manuscript.

**Funding:** Work in the laboratory of D.G.T. was supported, in part, by grants from the U.S National Institutes of Health (NIH) R01CA237027 and R01CA240290, the Prostate Cancer Foundation (PCF) Challenge Award, and by Roswell Park Alliance Foundation (RPAF), the George Decker Endowment, the Roswell Park NCI center grant P30CA016056. We also wish to acknowledge the NIH S10OD16450 grant support of IVIS Spectrum awarded to the Roswell Park Translational Imaging Shared Resource. Work in the laboratory of A.L.K. was supported, in part, by grants from the US NIH (1R01CA226259 and 1R01CA205420) and DOD (W81XWH2211085).

**Institutional Review Board Statement:** All animal-related studies in this study have been approved by our Institutional Animal Care and Use Committee (IACUC) at the Roswell Park Comprehensive Cancer Center (animal protocol# 1331 M and 1328 M).

**Informed Consent Statement:** Not applicable.

**Data Availability Statement:** The datasets used and/or analyzed in the study are available from the corresponding authors upon request.

**Conflicts of Interest:** The authors declare no conflicts of interest.

## References

1. Sartor, O.; de Bono, J.S. Metastatic Prostate Cancer. *N. Engl. J. Med.* **2018**, *378*, 645–657. [CrossRef]
2. Rice, M.A.; Malhotra, S.V.; Stoyanova, T. Second-Generation Antiandrogens: From Discovery to Standard of Care in Castration Resistant Prostate Cancer. *Front. Oncol.* **2019**, *9*, 801. [CrossRef]
3. Qin, J.; Liu, X.; Laffin, B.; Chen, X.; Choy, G.; Jeter, C.R.; Calhoun-Davis, T.; Li, H.; Palapattu, G.S.; Pang, S.; et al. The PSA(-/lo) prostate cancer cell population harbors self-renewing long-term tumor-propagating cells that resist castration. *Cell Stem Cell* **2012**, *10*, 556–569. [CrossRef]
4. Li, Q.; Deng, Q.; Chao, H.-P.; Liu, X.; Lu, Y.; Lin, K.; Liu, B.; Tang, G.W.; Zhang, D.; Tracz, A.; et al. Linking prostate cancer cell AR heterogeneity to distinct castration and enzalutamide responses. *Nat. Commun.* **2018**, *9*, 3600. [CrossRef] [PubMed]
5. Li, W.J.; Liu, X.; Dougherty, E.M.; Tang, D.G. MicroRNA-34a, Prostate Cancer Stem Cells, and Therapeutic Development. *Cancers* **2022**, *14*, 4538. [CrossRef] [PubMed]



6. Liu, X.; Li, W.; Puzanov, I.; Goodrich, D.W.; Chatta, G.; Tang, D.G. Prostate cancer as a dedifferentiated organ: Androgen receptor, cancer stem cells, and cancer stemness. *Essays Biochem.* **2022**, *66*, 291–303. [[CrossRef](#)] [[PubMed](#)]
7. Li, W.; Wang, Y.; Liu, R.; Kasinski, A.L.; Shen, H.; Slack, F.J.; Tang, D.G. MicroRNA-34a: Potent Tumor Suppressor, Cancer Stem Cell Inhibitor, and Potential Anticancer Therapeutic. *Front. Cell Dev. Biol.* **2021**, *9*, 640587. [[CrossRef](#)] [[PubMed](#)]
8. Zhang, L.; Liao, Y.; Tang, L. MicroRNA-34 family: A potential tumor suppressor and therapeutic candidate in cancer. *J. Exp. Clin. Cancer Res.* **2019**, *38*, 53. [[CrossRef](#)]
9. Zhang, G.; Tian, X.; Li, Y.; Wang, Z.; Li, X.; Zhu, C. miR-27b and miR-34a enhance docetaxel sensitivity of prostate cancer cells through inhibiting epithelial-to-mesenchymal transition by targeting ZEB1. *Biomed. Pharmacother.* **2018**, *97*, 736–744. [[CrossRef](#)]
10. Gaur, S.; Wen, Y.; Song, J.H.; Parikh, N.U.; Mangala, L.S.; Blessing, A.M.; Ivan, C.; Wu, S.Y.; Varkaris, A.; Shi, Y.; et al. Chitosan nanoparticle-mediated delivery of miRNA-34a decreases prostate tumor growth in the bone and its expression induces non-canonical autophagy. *Oncotarget* **2015**, *6*, 29161–29177. [[CrossRef](#)]
11. Liu, C.; Kelnar, K.; Liu, B.; Chen, X.; Calhoun-Davis, T.; Li, H.; Patrawala, L.; Yan, H.; Jeter, C.; Honorio, S.; et al. The microRNA miR-34a inhibits prostate cancer stem cells and metastasis by directly repressing CD44. *Nat. Med.* **2011**, *17*, 211–215. [[CrossRef](#)]
12. Yamamura, S.; Saini, S.; Majid, S.; Hirata, H.; Ueno, K.; Deng, G.; Dahiya, R. MicroRNA-34a modulates c-Myc transcriptional complexes to suppress malignancy in human prostate cancer cells. *PLoS ONE* **2012**, *7*, e29722. [[CrossRef](#)] [[PubMed](#)]
13. Chen, W.Y.; Liu, S.Y.; Chang, Y.S.; Yin, J.J.; Yeh, H.L.; Mouhieddine, T.H.; Hadadeh, O.; Abou-Kheir, W.; Liu, Y.N. MicroRNA-34a regulates WNT/TCF7 signaling and inhibits bone metastasis in Ras-activated prostate cancer. *Oncotarget* **2015**, *6*, 441–457. [[CrossRef](#)] [[PubMed](#)]
14. Alves-Fernandes, D.K.; Jasiulionis, M.G. The Role of SIRT1 on DNA Damage Response and Epigenetic Alterations in Cancer. *Int. J. Mol. Sci.* **2019**, *20*, 3153. [[CrossRef](#)] [[PubMed](#)]
15. Kojima, K.; Fujita, Y.; Nozawa, Y.; Deguchi, T.; Ito, M. MiR-34a attenuates paclitaxel-resistance of hormone-refractory prostate cancer PC3 cells through direct and indirect mechanisms. *Prostate* **2010**, *70*, 1501–1512. [[CrossRef](#)] [[PubMed](#)]
16. Corcoran, C.; Rani, S.; O'Driscoll, L. miR-34a is an intracellular and exosomal predictive biomarker for response to docetaxel with clinical relevance to prostate cancer progression. *Prostate* **2014**, *74*, 1320–1334. [[CrossRef](#)] [[PubMed](#)]
17. Dowdy, S.F. Overcoming cellular barriers for RNA therapeutics. *Nat. Biotechnol.* **2017**, *35*, 222–229. [[CrossRef](#)] [[PubMed](#)]
18. Segal, M.; Slack, F.J. Challenges identifying efficacious miRNA therapeutics for cancer. *Expert. Opin. Drug. Discov.* **2020**, *15*, 987–992. [[CrossRef](#)] [[PubMed](#)]
19. Abdelaal, A.M.; Kasinski, A.L. Ligand-mediated delivery of RNAi-based therapeutics for the treatment of oncological diseases. *NAR Cancer* **2021**, *3*, zcab030. [[CrossRef](#)]
20. Chen, Y.; Gao, D.Y.; Huang, L. In vivo delivery of miRNAs for cancer therapy: Challenges and strategies. *Adv. Drug Deliv. Rev.* **2015**, *81*, 128–141. [[CrossRef](#)]
21. Orellana, E.A.; Tenneti, S.; Rangasamy, L.; Lyle, L.T.; Low, P.S.; Kasinski, A.L. FolamiRs: Ligand-targeted, vehicle-free delivery of microRNAs for the treatment of cancer. *Sci. Transl. Med.* **2017**, *9*, eaam9327. [[CrossRef](#)] [[PubMed](#)]
22. Leamon, C.P.; Low, P.S. Folate-mediated targeting: From diagnostics to drug and gene delivery. *Drug Discov. Today* **2001**, *6*, 44–51. [[CrossRef](#)]
23. Kularatne, S.A.; Wang, K.; Santhapuram, H.K.R.; Low, P.S. Prostate-Specific Membrane Antigen Targeted Imaging and Therapy of Prostate Cancer Using a PSMA Inhibitor as a Homing Ligand. *Mol. Pharm.* **2009**, *6*, 780–789. [[CrossRef](#)]
24. Bravaccini, S.; Puccetti, M.; Bocchini, M.; Ravaioli, S.; Celli, M.; Scarpi, E.; De Giorgi, U.; Tumedei, M.M.; Raulli, G.; Cardinale, L.; et al. PSMA expression: A potential ally for the pathologist in prostate cancer diagnosis. *Sci. Rep.* **2018**, *8*, 4254. [[CrossRef](#)]
25. Sheehan, B.; Guo, C.; Neeb, A.; Paschalis, A.; Sandhu, S.; de Bono, J.S. Prostate-specific Membrane Antigen Biology in Lethal Prostate Cancer and its Therapeutic Implications. *Eur. Urol. Focus* **2021**, *8*, 1157–1168. [[CrossRef](#)]
26. Wang, F.; Li, Z.; Feng, X.; Yang, D.; Lin, M. Advances in PSMA-targeted therapy for prostate cancer. *Prostate Cancer Prostatic Dis.* **2022**, *25*, 11–26. [[CrossRef](#)] [[PubMed](#)]
27. He, L.; He, X.; Lim, L.P.; de Stanchina, E.; Xuan, Z.; Liang, Y.; Xue, W.; Zender, L.; Magnus, J.; Ridzon, D.; et al. A microRNA component of the p53 tumour suppressor network. *Nature* **2007**, *447*, 1130–1134. [[CrossRef](#)] [[PubMed](#)]
28. Chang, T.C.; Wentzel, E.A.; Kent, O.A.; Ramachandran, K.; Mullendore, M.; Lee, K.H.; Feldmann, G.; Yamakuchi, M.; Ferlito, M.; Lowenstein, C.J.; et al. Transactivation of miR-34a by p53 broadly influences gene expression and promotes apoptosis. *Mol. Cell* **2007**, *26*, 745–752. [[CrossRef](#)]
29. Raver-Shapira, N.; Marciano, E.; Meiri, E.; Spector, Y.; Rosenfeld, N.; Moskovits, N.; Bentwich, Z.; Oren, M. Transcriptional activation of miR-34a contributes to p53-mediated apoptosis. *Mol. Cell* **2007**, *26*, 731–743. [[CrossRef](#)]
30. Zhang, D.; Park, D.; Zhong, Y.; Lu, Y.; Rycaj, K.; Gong, S.; Chen, X.; Liu, X.; Chao, H.P.; Whitney, P.; et al. Stem cell and neurogenic gene-expression profiles link prostate basal cells to aggressive prostate cancer. *Nat. Commun.* **2016**, *7*, 10798. [[CrossRef](#)]
31. Rajan, P.; Sudbery, I.M.; Villasevil, M.E.; Mui, E.; Fleming, J.; Davis, M.; Ahmad, I.; Edwards, J.; Sansom, O.J.; Sims, D.; et al. Next-generation sequencing of advanced prostate cancer treated with androgen-deprivation therapy. *Eur. Urol.* **2014**, *66*, 32–39. [[CrossRef](#)]
32. Sharma, N.V.; Pellegrini, K.L.; Ouellet, V.; Giuste, F.O.; Ramalingam, S.; Watanabe, K.; Adam-Granger, E.; Fossouo, L.; You, S.; Freeman, M.R.; et al. Identification of the Transcription Factor Relationships Associated with Androgen Deprivation Therapy Response and Metastatic Progression in Prostate Cancer. *Cancers* **2018**, *10*, 379. [[CrossRef](#)]
33. Jeitner, T.M.; Babich, J.W.; Kelly, J.M. Advances in PSMA theranostics. *Transl. Oncol.* **2022**, *22*, 101450. [[CrossRef](#)]

34. Yao, V.; Berkman, C.E.; Choi, J.K.; O'Keefe, D.S.; Bacich, D.J. Expression of prostate-specific membrane antigen (PSMA), increases cell folate uptake and proliferation and suggests a novel role for PSMA in the uptake of the non-polyglutamated folate, folic acid. *Prostate* **2010**, *70*, 305–316. [[CrossRef](#)]
35. Maurer, T.; Eiber, M.; Schwaiger, M.; Gschwend, J.E. Current use of PSMA-PET in prostate cancer management. *Nat. Rev. Urol.* **2016**, *13*, 226–235. [[CrossRef](#)]
36. Liu, H.; Rajasekaran, A.K.; Moy, P.; Xia, Y.; Kim, S.; Navarro, V.; Rahmati, R.; Bander, N.H. Constitutive and antibody-induced internalization of prostate-specific membrane antigen. *Cancer Res.* **1998**, *58*, 4055–4060.
37. Ghosh, A.; Heston, W.D. Tumor target prostate specific membrane antigen (PSMA) and its regulation in prostate cancer. *J. Cell Biochem.* **2004**, *91*, 528–539. [[CrossRef](#)]
38. Flores, O.; Santra, S.; Kaittanis, C.; Bassiouni, R.; Khaled, A.S.; Khaled, A.R.; Grimm, J.; Perez, J.M. PSMA-Targeted Theranostic Nanocarrier for Prostate Cancer. *Theranostics* **2017**, *7*, 2477–2494. [[CrossRef](#)] [[PubMed](#)]
39. Beg, M.S.; Brenner, A.J.; Sachdev, J.; Borad, M.; Kang, Y.-K.; Stoudemire, J.; Smith, S.; Bader, A.G.; Kim, S.; Hong, D.S. Phase I study of MRX34, a liposomal miR-34a mimic, administered twice weekly in patients with advanced solid tumors. *Investig. New Drugs* **2017**, *35*, 180–188. [[CrossRef](#)] [[PubMed](#)]
40. Hong, D.S.; Kang, Y.-K.; Borad, M.; Sachdev, J.; Ejadi, S.; Lim, H.Y.; Brenner, A.J.; Park, K.; Lee, J.-L.; Kim, T.-Y.; et al. Phase 1 study of MRX34, a liposomal miR-34a mimic, in patients with advanced solid tumours. *Br. J. Cancer* **2020**, *122*, 1630–1637. [[CrossRef](#)] [[PubMed](#)]
41. Rajasekaran, A.K.; Anilkumar, G.; Christiansen, J.J. Is prostate-specific membrane antigen a multifunctional protein? *Am. J. Physiol. Cell Physiol.* **2005**, *288*, C975–C981. [[CrossRef](#)]
42. Evans, J.C.; Malhotra, M.; Guo, J.; O'Shea, J.P.; Hanrahan, K.; O'Neill, A.; Landry, W.D.; Griffin, B.T.; Darcy, R.; Watson, R.W.; et al. Folate-targeted amphiphilic cyclodextrin-siRNA nanoparticles for prostate cancer therapy exhibit PSMA mediated uptake, therapeutic gene silencing in vitro and prolonged circulation in vivo. *Nanomedicine* **2016**, *12*, 2341–2351. [[CrossRef](#)]
43. Jivrajani, M.; Nivsarkar, M. Ligand-targeted bacterial micelles: Futuristic nano-sized drug delivery system for the efficient and cost effective delivery of shRNA to cancer cells. *Nanomedicine* **2016**, *12*, 2485–2498. [[CrossRef](#)]
44. Patil, Y.; Shmeeda, H.; Amitay, Y.; Ohana, P.; Kumar, S.; Gabizon, A. Targeting of folate-conjugated liposomes with co-entrapped drugs to prostate cancer cells via prostate-specific membrane antigen (PSMA). *Nanomedicine* **2018**, *14*, 1407–1416. [[CrossRef](#)] [[PubMed](#)]
45. Xiang, B.; Dong, D.W.; Shi, N.Q.; Gao, W.; Yang, Z.Z.; Cui, Y.; Cao, D.Y.; Qi, X.R. PSA-responsive and PSMA-mediated multifunctional liposomes for targeted therapy of prostate cancer. *Biomaterials* **2013**, *34*, 6976–6991. [[CrossRef](#)] [[PubMed](#)]
46. Chen, Y.L.; Chang, M.C.; Huang, C.Y.; Chiang, Y.C.; Lin, H.W.; Chen, C.A.; Hsieh, C.Y.; Cheng, W.F. Serous ovarian carcinoma patients with high alpha-folate receptor had reducing survival and cytotoxic chemo-response. *Mol. Oncol.* **2012**, *6*, 360–369. [[CrossRef](#)] [[PubMed](#)]
47. Liu, C.; Ding, L.; Bai, L.; Chen, X.; Kang, H.; Hou, L.; Wang, J. Folate receptor alpha is associated with cervical carcinogenesis and regulates cervical cancer cells growth by activating ERK1/2/c-Fos/c-Jun. *Biochem. Biophys. Res. Commun.* **2017**, *491*, 1083–1091. [[CrossRef](#)] [[PubMed](#)]
48. Scaranti, M.; Cojocaru, E.; Banerjee, S.; Banerji, U. Exploiting the folate receptor alpha in oncology. *Nat. Rev. Clin. Oncol.* **2020**, *17*, 349–359. [[CrossRef](#)] [[PubMed](#)]
49. Zamarin, D.; Walderich, S.; Holland, A.; Zhou, Q.; Iasonos, A.E.; Torrisi, J.M.; Merghoub, T.; Chesebrough, L.F.; McDonnell, A.S.; Gallagher, J.M.; et al. Safety, immunogenicity, and clinical efficacy of durvalumab in combination with folate receptor alpha vaccine TPIV200 in patients with advanced ovarian cancer: A phase II trial. *J. Immunother. Cancer* **2020**, *8*, e000829. [[CrossRef](#)] [[PubMed](#)]
50. Moore, K.N.; Oza, A.M.; Colombo, N.; Oaknin, A.; Scambia, G.; Lorusso, D.; Konecny, G.E.; Banerjee, S.; Murphy, C.G.; Tanyi, J.L.; et al. Phase III, randomized trial of mirvetuximab soravtansine versus chemotherapy in patients with platinum-resistant ovarian cancer: Primary analysis of FORWARD I. *Ann. Oncol.* **2021**, *32*, 757–765. [[CrossRef](#)]
51. Kim, H.; Kim, M.W.; Jeong, Y.I.; Yang, H.S. Redox-Sensitive and Folate-Receptor-Mediated Targeting of Cervical Cancer Cells for Photodynamic Therapy Using Nanophotosensitizers Composed of Chlorin e6-Conjugated beta-Cyclodextrin via Diselenide Linkage. *Cells* **2021**, *10*, 2190. [[CrossRef](#)]
52. McGray, A.J.R.; Chiello, J.L.; Tsuji, T.; Long, M.; Maraszek, K.; Gaulin, N.; Rosario, S.R.; Hess, S.M.; Abrams, S.I.; Kozbor, D.; et al. BiTE secretion by adoptively transferred stem-like T cells improves FRalpha+ ovarian cancer control. *J. Immunother. Cancer* **2023**, *11*, e006863. [[CrossRef](#)]
53. Thomas, M.; Kularatne, S.A.; Qi, L.; Kleindl, P.; Leamon, C.P.; Hansen, M.J.; Low, P.S. Ligand-targeted delivery of small interfering RNAs to malignant cells and tissues. *Ann. N. Y. Acad. Sci.* **2009**, *1175*, 32–39. [[CrossRef](#)]
54. Tai, W.; Li, J.; Corey, E.; Gao, X. A ribonucleoprotein octamer for targeted siRNA delivery. *Nat. Biomed. Eng.* **2018**, *2*, 326–337. [[CrossRef](#)]
55. Pei, D.; Buyanova, M. Overcoming Endosomal Entrapment in Drug Delivery. *Bioconjug. Chem.* **2019**, *30*, 273–283. [[CrossRef](#)] [[PubMed](#)]
56. Dowdy, S.F.; Setten, R.L.; Cui, X.S.; Jadhav, S.G. Delivery of RNA Therapeutics: The Great Endosomal Escape! *Nucleic Acid Ther.* **2022**, *32*, 361–368. [[CrossRef](#)] [[PubMed](#)]

57. Gao, Y.; Li, Y.; Li, Y.; Yuan, L.; Zhou, Y.; Li, J.; Zhao, L.; Zhang, C.; Li, X.; Liu, Y. PSMA-mediated endosome escape-accelerating polymeric micelles for targeted therapy of prostate cancer and the real time tracing of their intracellular trafficking. *Nanoscale* **2015**, *7*, 597–612. [[CrossRef](#)] [[PubMed](#)]
58. Caron, N.J.; Quenneville, S.P.; Tremblay, J.P. Endosome disruption enhances the functional nuclear delivery of Tat-fusion proteins. *Biochem. Biophys. Res. Commun.* **2004**, *319*, 12–20. [[CrossRef](#)] [[PubMed](#)]
59. Chen, S.; Wang, S.; Kopytynski, M.; Bachelet, M.; Chen, R. Membrane-Anchoring, Comb-Like Pseudopeptides for Efficient, pH-Mediated Membrane Destabilization and Intracellular Delivery. *ACS Appl. Mater. Interfaces* **2017**, *9*, 8021–8029. [[CrossRef](#)]
60. Hassler, M.R.; Turanov, A.A.; Alterman, J.F.; Haraszti, R.A.; Coles, A.H.; Osborn, M.F.; Echeverria, D.; Nikan, M.; Salomon, W.E.; Roux, L.; et al. Comparison of partially and fully chemically-modified siRNA in conjugate-mediated delivery in vivo. *Nucleic Acids Res.* **2018**, *46*, 2185–2196. [[CrossRef](#)] [[PubMed](#)]
61. Abdelaal, A.M.; Sohal, I.S.; Iyer, S.; Sudarshan, K.; Kothandaraman, H.; Lanman, N.A.; Low, P.S.; Kasinski, A.L. A first-in-class fully modified version of miR-34a with outstanding stability, activity, and anti-tumor efficacy. *Oncogene* **2023**, *42*, 2985–2999. [[CrossRef](#)] [[PubMed](#)]
62. Bakht, M.K.; Yamada, Y.; Ku, S.Y.; Venkadakrishnan, V.B.; Korsen, J.A.; Kalidindi, T.M.; Mizuno, K.; Ahn, S.H.; Seo, J.H.; Garcia, M.M.; et al. Landscape of prostate-specific membrane antigen heterogeneity and regulation in AR-positive and AR-negative metastatic prostate cancer. *Nat. Cancer* **2023**, *4*, 699–715. [[CrossRef](#)] [[PubMed](#)]
63. Paschalis, A.; Sheehan, B.; Riisnaes, R.; Rodrigues, D.N.; Gurel, B.; Bertan, C.; Ferreira, A.; Lambros, M.B.K.; Seed, G.; Yuan, W.; et al. Prostate-specific Membrane Antigen Heterogeneity and DNA Repair Defects in Prostate Cancer. *Eur. Urol.* **2019**, *76*, 469–478. [[CrossRef](#)] [[PubMed](#)]
64. Sayar, E.; Patel, R.A.; Coleman, I.M.; Roudier, M.P.; Zhang, A.; Mustafi, P.; Low, J.Y.; Hanratty, B.; Ang, L.S.; Bhatia, V.; et al. Reversible epigenetic alterations mediate PSMA expression heterogeneity in advanced metastatic prostate cancer. *JCI Insight* **2023**, *8*, e162907. [[CrossRef](#)]
65. Sartor, O.; de Bono, J.; Chi, K.N.; Fizazi, K.; Herrmann, K.; Rahbar, K.; Tagawa, S.T.; Nordquist, L.T.; Vaishampayan, N.; El-Haddad, G.; et al. Lutetium-177-PSMA-617 for Metastatic Castration-Resistant Prostate Cancer. *N. Engl. J. Med.* **2021**, *385*, 1091–1103. [[CrossRef](#)]

**Disclaimer/Publisher’s Note:** The statements, opinions and data contained in all publications are solely those of the individual author(s) and contributor(s) and not of MDPI and/or the editor(s). MDPI and/or the editor(s) disclaim responsibility for any injury to people or property resulting from any ideas, methods, instructions or products referred to in the content.